HYDROGENIC SPECIES TRANSPORT ASSESMENTS IN CERAMIC ALUMINAS USED IN ITER ICRH H&CD AND DIAGNOSTIC SYSTEMS

Extending understanding and modelling capabilities through parametrical studies and sophisticate release-rate models

C. MORENO, L. A. SEDANO

Fusion Materials Research Unit
EURATOM-CIEMAT Fusion Association, Ed. 43 P0.04
Avda. Complutense 22, E-28040 Madrid

December 2006

HYDROGENIC SPECIES TRANSPORT ASSESMENTS IN CERAMIC ALUMINAS USED IN ITER ICRH H&CD AND DIAGNOSTIC SYSTEMS

Extending understanding and modelling capabilities through parametrical studies and sophisticate release-rate models

C. MORENO, L. A. SEDANO

Fusion Materials Research Unit
EURATOM-CIEMAT Fusion Association, Ed. 43 P0.04
Avda. Complutense 22, E-28040 Madrid

December 2006

Abstract

Ceramic insulators will be used in the ITER Heating and Current Drive and Diagnostics (H&CD/D) systems as opto-electronic vacuum windows or as feed-throughs. Their performance as materials could come modified by the intake of deuterium-tritium which amounts might be enhanced by ionising radiation effects. Such vacuum windows have a primary safety role as tritium confinement barriers. Tritium transport analyses have major implications on the design and safety assessments of ITER RF H&CD systems. As it is shown, refined tritium transport release-rate models together with detailed parametric studies can precise such assessments. In addition such modeling serves as conceptual framework to quantify precise impact of underlying phenomena (ex. radiation-enhanced diffusion or potential effects of radiation damage on tritium transport through the Vacuum Window) and its final impact on main transport parameters of interest for VW design: permeation flux and D/T inventories. In the present work it has been shown how, for electric implantation of ionized D,T in the VW being the major source for isotopes intake, an hybrid recombination/radiation enhanced diffusion regime determine H-isotopes transport kinetics in the window. Precise values for permeation fluxes and inventories are provided from solution of mass transport equations. Near and medium term work planning is advanced.

Resumen

En ITER se van a usar aislantes cerámicos en las ventanas opto-electrónicas los sistemas de calentamiento y diagnóstico y en pasamuros. Su funcionamiento como materiales podría verse alterado por la incorporación de deuterio-tritio que puede verse realzada por efectos ionizantes de la radiación. Dichas ventanas tienen un papel primario de seguridad como barreras de confinamiento de tritio. Los análisis de transporte de tritio tienen implicaciones principales sobre el diseño y las evaluaciones de seguridad de sistemas de calentamiento por rf en ITER. Como se demuestra, los modelos refinados de tasa de liberación de transporte de tritio juntos con estudios paramétricos detallados pueden precisar tales evaluaciones. Además tal modelado sirve como marco conceptual para cuantificar el impacto exacto de los fenómenos implicados en el transporte (la difusión ejemplo realzada por radiación o los efectos potenciales de daño de radiación sobre el transporte de tritio en la Ventana) y su impacto final sobre los parámetros principales de transporte de interés para el diseño de VW: flujo de permeación e inventarios de D/T. En este trabajo se muestra como, la implantación de campo eléctrico del D/T ionizado, fuente principal para la entrada de isótopos en la ventana, es una combinación recombinacion/difusión la que determina la cinética de transporte de isótopos en la ventana. Se proporcionan valores exactos para flujos de permeación e inventarios por solución de ecuaciones de transporte. Se anticipa el trabajo previsto a corto y medio plazo.

Contents

List of Figures

List of Tables

1. Introduction

In ITER, the vacuum windows (VW) have a main role in the security as primary barrier of tritium confinement. Therefore it is necessary to make a good analysis of how the reactor environment affects to the materials that compose it. The first problems come with the hydrogenic species transport. High hydrogen isotope concentrations can modify the mechanical properties and change the VW operation time. The accumulation of hydrogenic species (H') also modifies the opto-electronic properties of the insulators used in the windows. It should be added radiation can potentially increase the adsorption-desorption and (H') diffusion rates in the material. Furthermore, radiation damage modifies the material bulk trapped inventories by increasing steady trapping centre concentrations. Hence, there is a present effort developing tools to model the VW from the real data of available tests. In CIEMAT labs a broad program to quantify radiation effects in insulating ceramics is developed where this work is included.

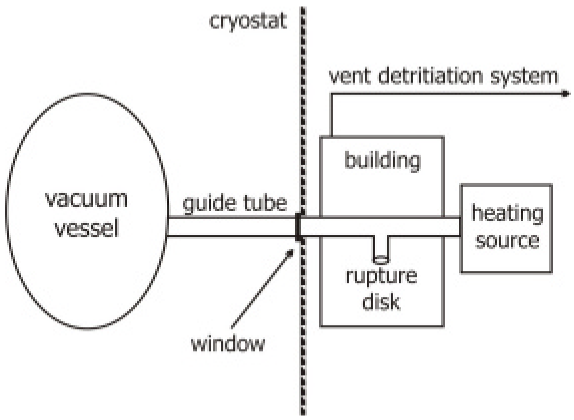

Figure 1. RF vacuum window position in ICRH Transmission Line and functional safety.

The material to study is the aluminum oxide Al_2O_3, both monocrystal (Sapphire) and polycrystal. Alumina is one of the candidates along with beryllium oxide to constitute the Ion Cyclotron Radiation Heating (ICRH) vacuum window, although the hydrogen transport and radiation effects existing database in diverse types of alumina is poor and needs to be extended. With this work is expected to make a parametric calculation determining what are the values which influence in the window optimization and must be experimentally measured to fit the design;

evaluating the permeation fluxes, trapped/solved inventories and characteristic times of the processes. This requires a complex exercise of thermal, electromagnetic and effects radiation characteristics connection for the window material.

The impossibility to anticipate experiments at reactor conditions like ITER makes necessary the simulation tools development to qualify the final designs. The TMAP7 code model the hydrogen isotope transport, which is adapted to the necessary calculation for the window analysis. It is advisable to justify a simplified model of the VW, both geometric and physical, which fits inputs to the ITER operational scene without losing precision. This will include:

- D/T gas species characteristics (ionization and disassociation degrees) facing the VW from pulsed-plasma first wall neutrals [1] under Transmission Line (TL) molecular conductance,
- VW thermal design characteristics [2] (temperature and gradients),
- VW local electromagnetic working field EB parameters [2] determining H-isotopes electro-implantation characteristics in the VW, and
- Radiation parameters (ionizing/total cumulated and dose rates [3, 4].

The set of main primary parameters entering in the release-rate model (RRM) are identified. The available isotopes´ database within application ranges for those magnitudes and main unknowns are summarized. Reference ranges of permeating fluxes and D/T solved/trapped inventories across/at VW-alumina windows together with parametric assessment covering range of interest in ITER will be later carried out.

Through a wide parametric range of VW working environment conditions, permeation fluxes are seen to be below Design Requirements Guideline [7] safety limits in ITER. Total mobile and trapped hydrogenic species inventories cover a wide parametric range for given radiation-enhanced and surface parameters.

2. Analyses

2.1. ICRH general lay-out: ITER VW DGR and design specifications

VW are conceived as transmission windows for RF voltage of 50 kV peak with 60 MHz for maximum 3000 s discharge durations for long pulse. The design specifications for the VW have been assumed from [2]. A coaxial line on the antenna side of the window assembly is directly connected to the chamber vacuum through an approx. 10 m duct. Ultimate designs are today under final qualification for ITER. VW upgrades can consider double windows or cooling with/without pumping of intermediate septa volumes. For present assessments is close to that assumed for ICRH VW design [4] with minimum modifying assumptions.

In this work, a single window design is assumed. An artistic view of VW is shown in Figure 2.

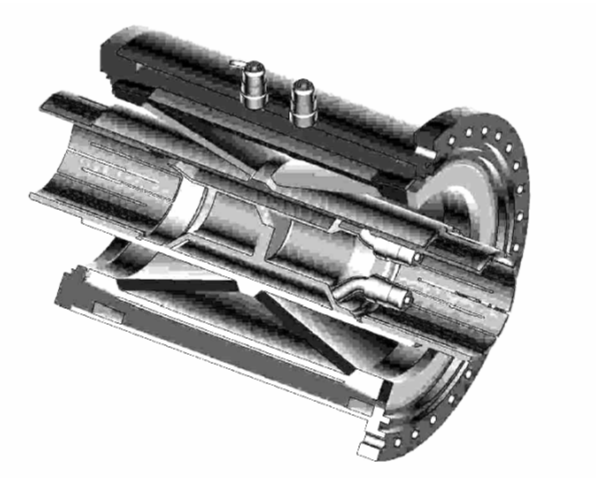

Figure 2: Radio-frequency vacuum ICRH window reference design (courtesy from [4]).

2.2 Simplified VW model

2.2.1 Ranges D/T ionic species plasma pulses facing the VW

Figure 3 shows assumptions on D_2/T_2 VW neutrals partial pressures conservatively assumed between 10-100 Pa at the ITER first wall. At such low neutral species partial pressures, molecular conductance through lines drives to a neutral pressure drop facing VW of few percentiles (~ 3 %) and synchronous with plasma pulses. DT isotopic ratio is computed from equilibrium constant [9]. At the TL operational conditions of pressure and temperatures the free gas atomic dissociation can be assumed as negligible.

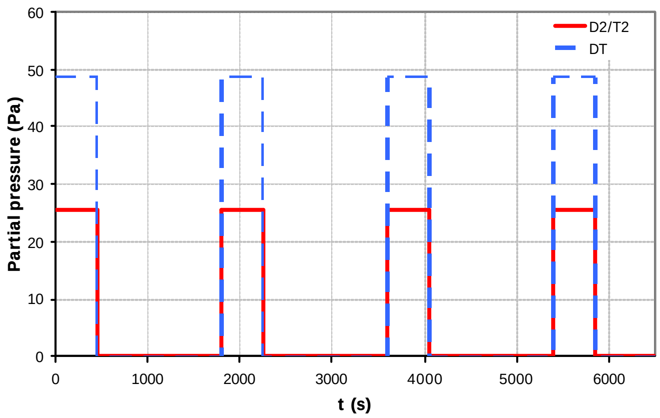

Figure 3: Equivalent neutral p. p. facing the VW assuming conservatively 100 Pa at the First Wall.

Ionisation degree of gas derived from the use of the most simple equilibrium model (ex. Saha equation):

$$n^2{}_i / n_n = \left[2p m_e kT / h^2\right]^{3/2} \exp(-U / b) \quad (1)$$

where b input is directly related with ionising dose replacing molecular thermal energy, drives to assumptions of high degree of ionisation (> 95%) of the molecular species. Radiation doses make gas ionisation very effective and the gas species facing the window should be assumed as fully ionised; a conservative assumption.

2.2.2 VW electromagnetic environing parameters

RF electrical field (50 kV peak, $E_{\perp}$: 1.85 MV/m, $E_{||}$: 0.60 MV/m) values would breed keV oscillating (60 MHz) ions impacting on the VW surface (Figure 4). While, in the ceramic, the tangential field is roughly the same as in the vacuum, the normal field is reduced in comparison with the tangential field by the ratio of the length along the ceramic and radial distance between the outer and inner conductors, roughly by a factor 3. Therefore, an isotopic implantation profile enters as interfacial flux input condition in the transport assessments. SRIM2003 code [10] capabilities have been used for these assessments (Figure 5).

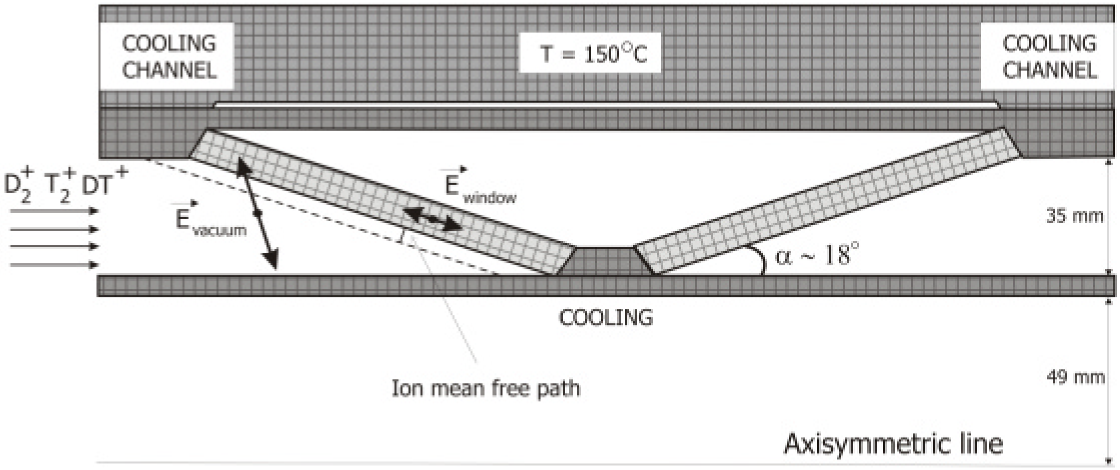

Figure 4: RF local electric field geometry determining ion sticking.

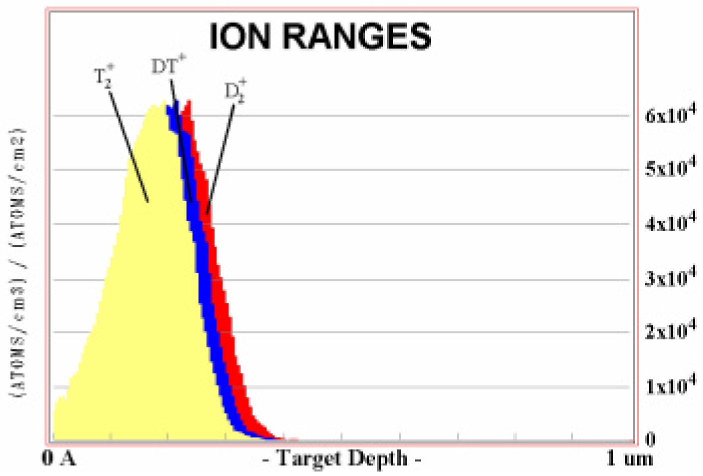

Figure 5. Distribution ranges for implanted ions in Al_2O_3 VW.

Charged particle bombardment is foreseen to cause oxygen ions ejection from the alumina, reason to believe in a loss of insulating properties in the course of time.

2.2.3 Thermal inputs

VW conductor is actively cooled (150º C). The high Ti,Cu and inter-metalic welds thermal conductivity together with radiation effects induces high degree of thermal homogeneity in the windows minimizing the thermal stresses. Heating of impinging ions at the TL/VW side and active cooling in intermediate septa volume can justify a stable thermal difference below 1 degree across the VW (i.e.: gradient values ~ 100 ºC/m). Thermo-diffusion effects on H-species transport (Ludwig-Soret effects) are assessed here following assuming as reference value such thermal gradient.

3. Release rate model

3.1 Initial scheme

From the most simplified TL/ionised gas/VW model and under the local electric field distribution conditions, the ion impinging ?$_i$ fluxes are rate-limited by the species molecular self-diffusion in the TL:

$$f_i = \frac{p_i s \cos(2a)}{\sqrt{2pm_i kT}} \qquad (2)$$

Under radiation operational conditions the driving forces for H-species transport through insulators are kinetically limited by transport processes at the VW surface and those at the VW ceramic bulk:

(1) mobile concentrations gradients (*Fick* flux),
(2) thermal gradients (*Ludwig-Soret* flux),
(3) electric potential field gradient (*Nerst-Einstein* electromigration flux),
(4) tensional stress field gradients.

Two different balanced flux schemes should be considered during plasma pulse operation (RF heating in force) and during plasma dwell time.

During (450 s or 3000 s) RF heating, the net flux at TL/VW interface is the result of balance between the implantation flux induced by local electric field (see Section 2.2.2.), an inwards diffusion flux and recombination fluxes at surfaces from backward flux. Compared with any of the characteristic transport times of the processes involved, the implanted ion stopping times (net ions implantation time) are 1-2 orders of magnitude shorter. In this sense implantation can be assumed as quasi-instantaneous. It can be assumed that during RF heating all the recycled amounts by recombination keeps available at the interface to be re-implanted by the local field.

During RF shut-down period (dwell time, 1350 s for short or 9000s for long pulses) the net flux of the previously implanted concentration is the balance between diffusion flux and recombination (Figure 6).

The complete set of equations describing the phenomenological release rate model for transport is given hereafter.

3.2 Phenomena, describing equations and key parameters

Even if hydrogen molecular states in alumina can not be thermodynamically precluded, hydrogenic species creates, once stopped, atomic populations within the material. Two species D and T (*i* subindex, 1, 2 respectively) are considered.

General transport equation for total concentration of specie *i*, net flux J_i and total source distribution in the material G_i the material writes as:

$$\frac{\partial c_i(x,t)}{\partial t} = -\frac{\partial J_i(x,t)}{\partial x} + G_i(x,t) \qquad (3)$$

with:

$$G_i(x,t) = G_{iI}(x,t) + G_{iN}(x,t) \qquad (4)$$

for x = (0,d) applying for TL/VW interfaces.

The contribution $G_{iN}(x,t)$ coming from transmutation $G_{iN}(x,t) = \{n(A,B)p, n(A',B')D\}$ can be neglected and G_i is mainly due to interfacial implantation:

$$G_{il}(x,t) = \Phi_i (1-R_i) \mathrm{P}_i (x,t) \qquad (5)$$

(R_i is the reflection coefficient of impinging ions in alumina: few percent at KeV energies at an angle of 18º, P_i(x, t) is the implantation distribution, and Φ_i is the flux impinging the window. SRIM2003 results (Figure 5) are used as input for implantation distribution.

Modelling of hydrogenic species transport in the VW should consider both, soluted mobile (s index) and trapped concentrations (t index):

$$c_i(x,t) = c_{is}(x,t) + c_{it}(x,t) \qquad (6)$$

then:

$$\frac{\partial c_{is}(x,t)}{\partial t} = -\frac{\partial J_i(x,t)}{\partial x} - \frac{\partial c_{it}(x,t)}{\partial t} + G_{il}(x,t) \qquad (7)$$

A mass-balance equation between trapped and mobile concentrations is commonly written following neutron capture analogy, trapping rates proportional to mobile and non-occupied trap and de-trapping proportional to occupation time with Boltzmann factor:

$$\frac{\partial c_{ti}(x,t)}{\partial t} = 4pR_T ND_i \left[c_{si}(c_T - \sum_{j=1}^{s} c_{tj}) - mc_{ti} \exp(-E_T / kT) \right] \qquad (8)$$

Taking into account the set of transport driving forces considered, the net flux is written as:

$$J_i(x,t) = -D_i \left(\frac{\partial c_{is}(x,t)}{\partial x} + c_{si} \frac{Q_i}{kT^2} \frac{\partial T(x,t)}{\partial x} \pm \frac{Z_i^* c_{si}(x,t) E}{kT} \right) \qquad (9)$$

Tensional stress effects on transport not considered. Flux at surface is a net balance between gas dissociation (not in force during RF operation and negligible during RF dwell periods) and atomic recombination at surface:

$$J_i(x=0,d) = (-1)^h \sum_{j=1}^{s} (K_r)_{ij} c_{si} c_{sj} \qquad (10)$$

Following the analogy for endo-thermal absorbers ($-E_S < 0$), (Figure 7) the recombination rate constant for species are written as:

$$(K_r)_{ij} = \frac{4C_0 s}{N\sqrt{(m_i + m_j)T K_{s0}^2}} \exp\{(E_s - E_d)/kT\} \qquad (11)$$

with C_0 being a constant $2.635 \cdot 10^{24} molec \cdot \sqrt{uma} \cdot \sqrt{K} \cdot Pa^{-1} \cdot s^{-1} \cdot m^{-2}$, K_{s0} solubility pre-exponential factor, $-E_s$, $-E_d$ solution and diffusion energies and ? the sticking factor characteristic for the material surface.

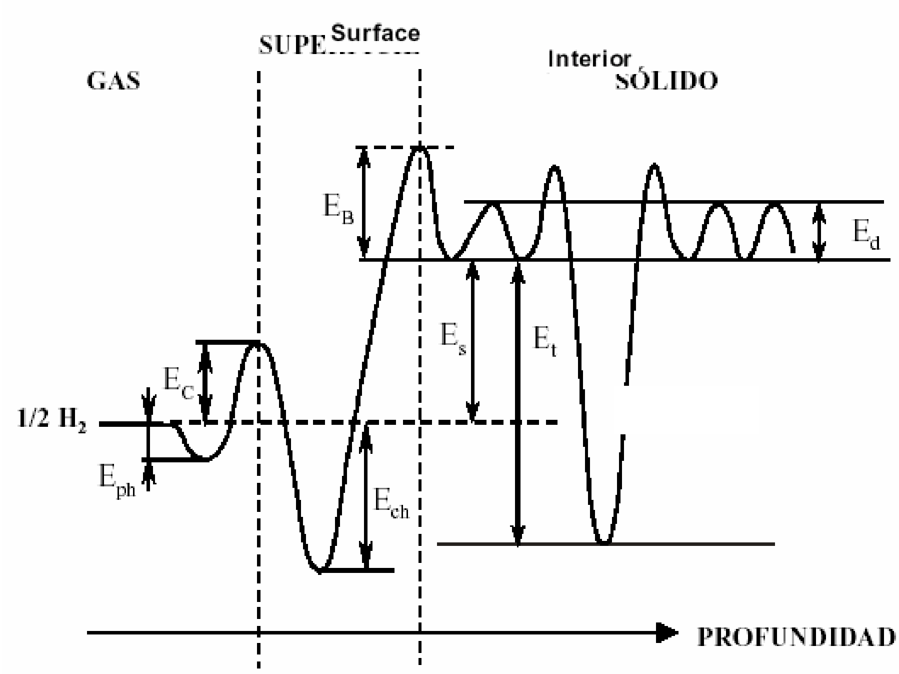

Figure 6: Thermal gas-ceramic surface energy diagram. As endothermal absorber ($-E_s < 0$) alumina shows low chemisoprtion $-E_{ch}$ energies and high surface barrier energies E_B.

Hence the primary transport parameters in the model are:

- diffusion coefficient, D_i
- surface sticking factor: σ
- heat for thermo-transport : Q_i
- net electro-migration charge of the hydrogenic specie: $0 < Z^*_i \leq 1$.

Classical isotopic dependence, i.e.: isotopic effect on jumping rate frequencies of H atoms in the material lattice for diffusion coefficients: $D_i = D_0 m_i^{-1/2} \exp(-E_d / kT)$ is assumed.

The main material constitutional parameters entering as input in transport model being: the material mass/atomic densities, *r (N)*, the trap radius R_T, the coordination number m, and trap energies: E_T.

The model proposed [6] is a generalisation of tritium transport model proposed in the past by [13] including species electro-migration and couplings between transport driving forces.

3.3 Database for sapphire and polycrystalline Al_2O_3

Generally speaking, the hydrogen transport database in diverse types of alumina is poor and needs to be extended.

Out-of-irradiation measurements carried out during sixties anticipated low thermal diffusivity of hydrogen in diverse aluminae with typical values twenty orders of magnitude lower (≈ 10^{-40} m^2s^{-1}) than in metals at VW working temperatures [11, 12]. Intrinsic values derived from measured permeation reduction factors of pack cemented or plasma spray alumina coatings [14] show, for diffusion-limited regimes, a global range agreement with pioneer measurements.

Several diffusion and permeability measurements under ionising radiation show radiation-enhanced diffusion/permeation trends. In [15] the modelling of D_2^+, D_3^+ 50 keV ion beam irradiation implantation profile in sapphire and WESGO alumina needed diffusion coefficient values twenty orders of magnitude higher than thermal ones to explain profiles. Values of sticking coefficients (σ) suggested for such ion implantation test was 0.001.

Al_2O_3	D_0 m^2/s	E_d eV	K_{s0} mol $m^{-3}Pa^{-0.5}$	E_s eV	Ref.
Sapphire	3.3×10^{-4}	2.48			[11]
T_2-WESGO®	7.3×10^{-6}	1.90			[11]
D_2			5.9	0.78	[12]
Transport parameters					
C_T (%)	0.01-0.03				[15]
E_T (eV)	0.71				
K_r (m^4/s)	5×10^{36} ?or $1<\sigma?\ 10^{-5}$				

Table I: Assumed hydrogenic species transport database in sapphire and policrystalline alumina [11, 12 and 15].

Recent *time-lag* D_2 measurements in sapphire, DERANOX© reports anomalous comparative irradiated/non-irradiated pressure drop under ionising radiation and, within 1-2 orders of magnitude, increase of measured fluxes [16]. A new experimental campaign has been undertaken to systematically quantify by modelling such observed trends.

No thermo-transport data for Hydrogen in alumina (*Q* values) is known. For parametrical modelling we have as closer numerical reference *Q* values for metals. As endothermal absorber $Q < 0$, thermo-diffusion makes H atoms to move naturally to hotter VW face. For the modelling of the TL/VW the non-inclusion of thermal gradients is conservative for fluxes and inventories.

As a difference with metals, the net electro-migration charge of the hydrogenic specie: Z^*_i within the insulator under high ionization field can be assumed close to 1.

The most reliable data for alumina used as reference input for present assessments is reported in Table 2. Tentative range values for neutron-induced trap centres, assumed constant along windows operational life-time are: 0.01 and 0.03 with 1 diffusion trap at maximum energy of 0.71eV.

4. Computations, parametric runs and results

The release rate model has been implemented in the numerical tool TMAP7 [5]. Electromigration flux, not explicitly computable by TMAP7 code has been included, at an imposed average temperature, exploiting the formal analogies existing between thermo-diffusion and electro-migration: a variable temperature gradient $z_i^* \bar{T} Q_i^{-1}$ times the RF electric field values. From this approach it could be inferred that variable polarisation of the RF neutralize effects on transport in the direction of the concentration gradients. Electric field distribution and field variable polarisation would homogenize migrating concentration along window axial direction, making 1-dimensional adaptation in TMAP7 accurate.

The main results proposed are shown in Figure 8. Values of D, T tritium inventories ranging orders of magnitude are obtained for several radiation enhanced diffusivity values, both short and long pulses. Typical profiles are shown in Figure 9. Accordingly, the computed tritium activity transfer values are well below ITER DRG [7].

Short pulses

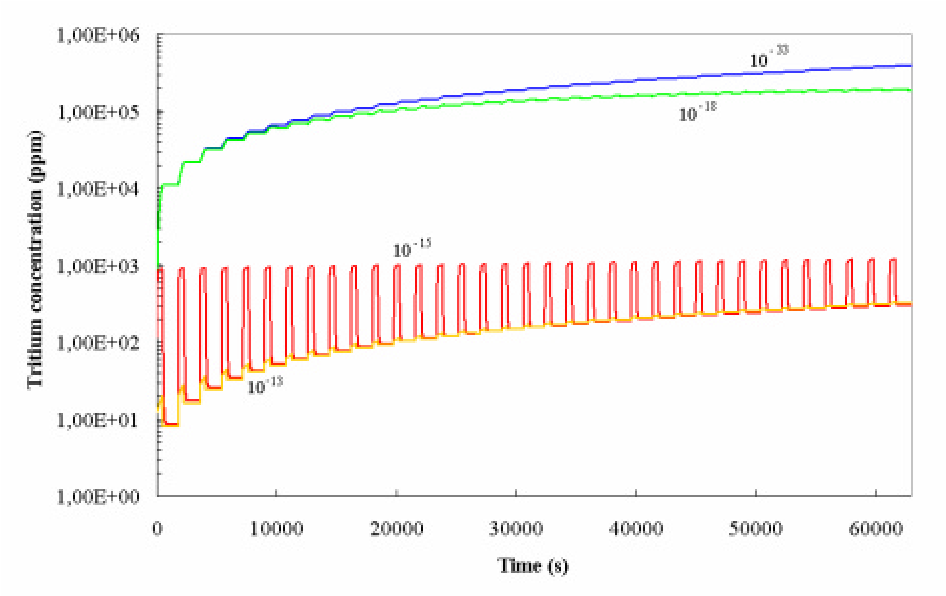

(a)

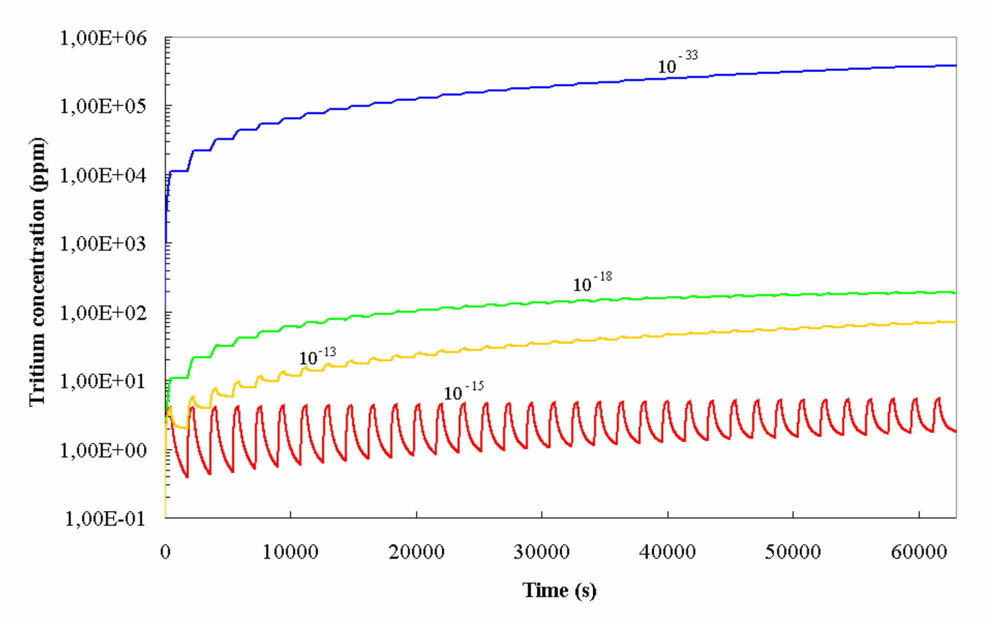

(b)

Figure 7a: Tritium total (mobile + trapped) concentrations parameter cases (a): σ: 10^{-2}, (b): σ: 10^{-5}.

Long pulses

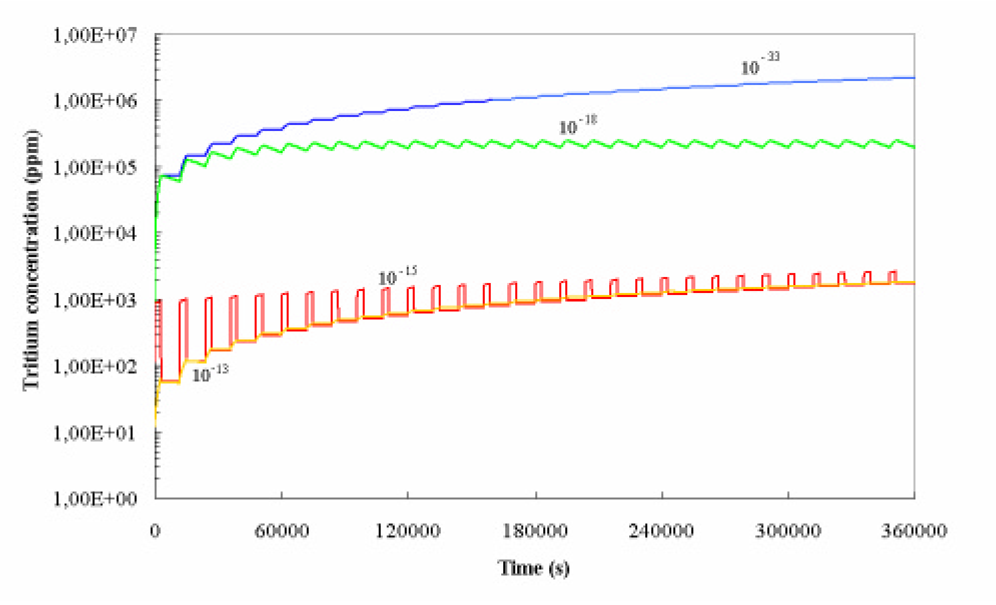

(a)

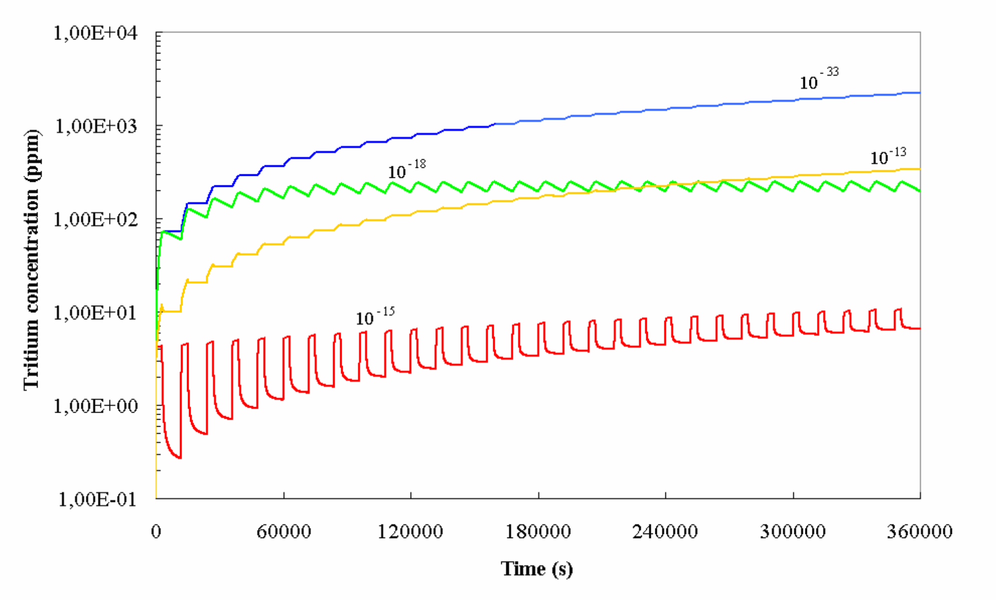

(b)

Figure 8b: Tritium total (mobile + trapped) concentrations parameter cases (a): σ: 10^{-2}, (b): σ: 10^{-5}.

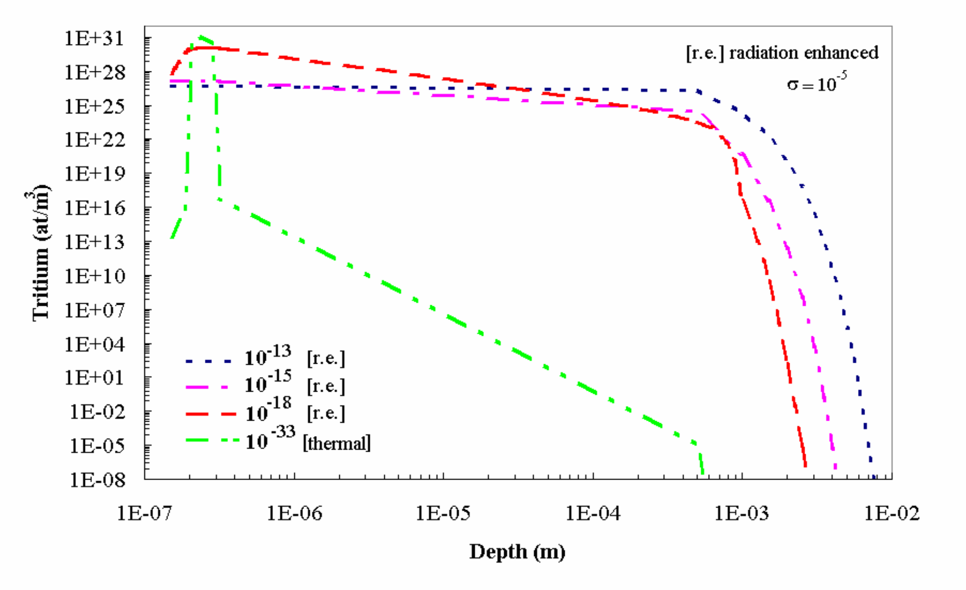

Figure 9: Tritium mobile concentration profiles in the VW.

5. Discussion and concluding remarks

Physical operational conditions of a generic alumina VW of ICRH system in ITER have been analysed. A phenomenological release-rate transport model has been formulated and adapted to TMAP7 1-dimensional finite modelling tool.

The results show how combined surface/radiation-rate regimes determine the species transport behaviour in the VW. These depend on the characteristic times, both diffusion and recombination, of the processes: $t_D = x^2/D$ and $t_R = x/K_r C$ respectively (Figure 10). Radiation-enhanced diffusion "through" competes with radiation enhanced diffusion "back" with shorter pathways for recombination-desorption back the TL.

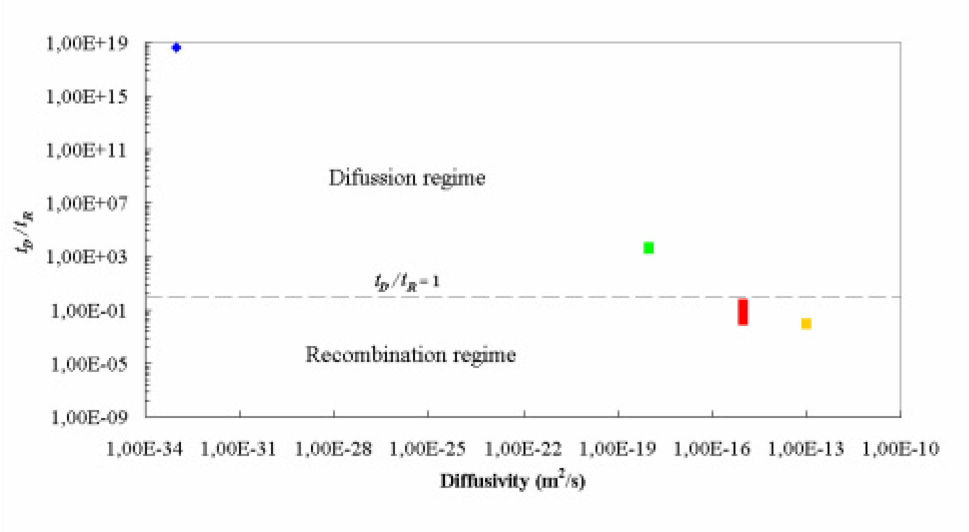

Figure 10: Characteristic times ratio vs. diffusivity.

As it can be verified in the Figures 8 and 10, the minimum of tritium concentration is for $t_D = t_R$, therefore a good qualification of the surface and under radiation diffusivity allows to choose an optimal window design. Experimental priorities are seen to be concentrated in precise quantifications of radiation-enhanced diffusion phenomenon with the mastering of surface roughness characteristics: σ values.

6. Near and medium-term work planning

Tritium transport analyses have major implications on the design and safety assessments of ITER RF H&CD systems. As has been shown, refined tritium transport release-rate models together with detailed parametric studies can precise such assessments. In addition such modeling can serve as conceptual framework to quantify precise impact of underlying phenomena (ex. radiation-enhanced diffusion or potential effects of radiation damage on tritium transport through the Vacuum Window) and its final impact on main transport parameters of interest for VW design: permeation flux and resilient D/T inventories. In the present work it has been shown how, for electric implantation of ionized D,T in the VW being the major source for isotopes intake, an hybrid *recombination/radiation enhanced diffusion* regime determine H-isotopes transport kinetics in the window.

Additionally the present refined release rate models are useful to establish, through sophisticated numerical analyses, the prospective targets of experimental activity generating the inputs needed in appropriate ranges. For the identified hybrid *recombination/radiation enhanced diffusion* regime main parameters of interest for experimental studies are:

- the final range of radiation enhanced diffusion factor enhancement,
- material surface constants (disassociation and recombination) entering in recombination rate constants (s: sticking coefficient),
- nominal values for radiation-induced trap concentrations c_T and trapping well´s energies E_T.

Correlations between known possible radiation-induced defect structures in Al_2O_3 and related E_T values seem of theoretical interest for near term investigations. Such correlations can also be established through well known procedures by transient experiments. According to ranges such experiments are very demanding in terms of experimental precision. The type of test and experimental capabilities needed will be detailed investigated in the near future.

The maximum design precision of inputs for D/T release rate can be obtained through the use of advanced computing tools. MCNPx tools (providing detailed neutron and charged particles transport analyses) are used to precise input values for precise damage computation at the Al_2O_3 VW using actual design inputs in ITER. A net computation of c_T value is in the short term scope of this work. As an extension to the work is expected to analyze the window infringed damage under radiation conditions in the operation time; evaluating with the neutron transport tool, MCNPX, the possible interactions with the alumina lattice and obtaining the consequences with SRIM2003 code [10].

The developed release-rate model and its implementation for the analysis of other VW/H&CD systems (ECRH, LHRH feedthroughs) is expected for the near future. Use of phenomenological release rate model to model real fusion data (real data is available from D/T experiments at JET and TFTR fusion machines) can be considered as medium term activity.

Appendix A. TMAP7 File Example

```
title input
  ITER ICRF Alumina Window, sticking 10-2, Long Pulse, no enhanced-radiation
end of title input
$
main input
  dspcnme=d,t,end
  espcnme=d2g,t2g,dtg,end
  segnds=27,end
  nbrencl=2,end
end of main input
$
enclosure input
$
start func,1,end
$ Vacuum
    etemp=const,423.0,end
    esppres=d2g,1.0e-4,t2g,1.0e-4,dtg,1.0e-4,end
    evol=1.594e-1,end
start func,2,end
$ Vacuum
    etemp=const,423.0,end
    esppres=d2g,1.0e-4,t2g,1.0e-4,dtg,1.0e-4,end
    evol=1.5e-3,end
end of enclosure input
$
thermal input
$  Segment 1  -  Alumina Window
start thermseg,end
    delx=0.0,1.5e-7,0.36e-7,0.2e-7,2*0.38e-7,20*0.0005,0.0,end
    tempd=27*423.0,end
end of thermal input
$
$
diffusion input
$  Segment 1  -  Alumina Window
start diffseg,end
    nbrden=2.3354e28,end
    concd=d,const,0.0,t,const,0.0,end
    trapping=ttyp,1,tconc,const,0.02,tspc,d,alphr
    equ,4,alpht,equ,6,ctrap,const,0.0,tspc,t,alphr,equ,5,alpht,equ,6
    ctrap,const,0.0,end
    dcoef=d,equ,2,t,equ,1,end
    qstrdr=d,const,0.0,t,const,0.0,end
    srcsd=d,tabl,1,srcpf,2*0.0,0.5,1.0,0.5,22*0.0
    t,tabl,2,srcpf,2*0.0,0.5,1.0,0.5,22*0.0,end
    difbcl=ratedep,encl,1
       spc,d
             exch,d2g,ksubd,const,0.0
                  d,ksubr,const,5.0e-35
             exch,dtg,ksubd,const,0.0
                  t,ksubr,const,5.0e-35
       spc,t
             exch,t2g,ksubd,const,0.0
                  t,ksubr,const,5.0e-35
             exch,dtg,ksubd,const,0.0
                  d,ksubr,const,5.0e-35,end
    difbcr=ratedep,encl,2
       spc,d
             exch,d2g,ksubd,const,0.0
                  d,ksubr,const,5.0e-35
             exch,dtg,ksubd,const,0.0
                  t,ksubr,const,5.0e-35
       spc,t
             exch,t2g,ksubd,const,0.0
                  t,ksubr,const,5.0e-35
             exch,dtg,ksubd,const,0.0
                  d,ksubr,const,5.0e-35,end
    surfa=1.594e-2,end
end of diffusion input
$
```

```
$
equation input
$
$ (1) Diffusivity of T in Al2O3 [Fowler,Journal of The American Ceramic Society,
$ 60, 155-161 (1977)]
y=3.3e-4*exp(-2.48/8.625e-5/temp),end
$
$ (2) Diffusivity of D in Al2O3 [Fowler,Journal of The American Ceramic Society,
$ 60, 155-161 (1977)]
y=4.04e-4*exp(-2.48/8.625e-5/temp),end
$
$ (3) Solubility of T,D in Al2O3
$(T.S. Elleman, R.A. Causey, D.R. Chari, P. Feng, R.M. Roberts, K. Verghese,
$L.R. Zumwalt, Tritium Diffusion in Nonmetallic Solids of Interest for Fusion
$Reactors, Annual Progress Report,ORO-4721-6 (1977)]
y=5.9*exp(-0.785/8.625e-5/temp),end
$
$ (4) Trap release rate (1/s)
y=1e13*exp(-0.7/8.62e-5/temp),end
$
$ (5) Trapping rate coefficient of T in Al2O3 [Fowler,J. of The American Ceramic Society,
$ 60, 155-161 (1977)]
y=2.6969e15*exp(-2.48/8.625e-5/temp),end
$
$ (6) Trapping rate coefficient of D in Al2O3 [Fowler,J. of The American Ceramic Society,
$ 60, 155-161 (1977)]
y=3.301e15*exp(-2.48/8.625e-5/temp),end
$
end of equation input
$
$
table input
$ (1) Flux history of D in Enclosure 1
0.0,1.569e22,3000.0,1.569e22,3001.0,0.0,12000.0,0.0
12001.0,1.569e22,15000.0,1.569e22,15001.0,0.0,24000.0,0.0
24001.0,1.569e22,27000.0,1.569e22,27001.0,0.0,36000.0,0.0
36001.0,1.569e22,39000.0,1.569e22,39001.0,0.0,48000.0,0.0
48001.0,1.569e22,51000.0,1.569e22,51001.0,0.0,60000.0,0.0
60001.0,1.569e22,63000.0,1.569e22,63001.0,0.0,72000.0,0.0
72001.0,1.569e22,75000.0,1.569e22,75001.0,0.0,84000.0,0.0
84001.0,1.569e22,87000.0,1.569e22,87001.0,0.0,96000.0,0.0
96001.0,1.569e22,99000.0,1.569e22,99001.0,0.0,108000.0,0.0
108001.0,1.569e22,111000.0,1.569e22,111001.0,0.0,120000.0,0.0
120001.0,1.569e22,123000.0,1.569e22,123001.0,0.0,132000.0,0.0
132001.0,1.569e22,135000.0,1.569e22,135001.0,0.0,144000.0,0.0
144001.0,1.569e22,147000.0,1.569e22,147001.0,0.0,156000.0,0.0
156001.0,1.569e22,159000.0,1.569e22,159001.0,0.0,168000.0,0.0
168001.0,1.569e22,171000.0,1.569e22,171001.0,0.0,180000.0,0.0
180001.0,1.569e22,183000.0,1.569e22,183001.0,0.0,192000.0,0.0
192001.0,1.569e22,195000.0,1.569e22,195001.0,0.0,204000.0,0.0
204001.0,1.569e22,207000.0,1.569e22,207001.0,0.0,216000.0,0.0
216001.0,1.569e22,219000.0,1.569e22,219001.0,0.0,228000.0,0.0
228001.0,1.569e22,231000.0,1.569e22,231001.0,0.0,240000.0,0.0
240001.0,1.569e22,243000.0,1.569e22,243001.0,0.0,252000.0,0.0
252001.0,1.569e22,255000.0,1.569e22,255001.0,0.0,264000.0,0.0
264001.0,1.569e22,267000.0,1.569e22,267001.0,0.0,276000.0,0.0
276001.0,1.569e22,279000.0,1.569e22,279001.0,0.0,288000.0,0.0
288001.0,1.569e22,291000.0,1.569e22,291001.0,0.0,300000.0,0.0
300001.0,1.569e22,303000.0,1.569e22,303001.0,0.0,312000.0,0.0
312001.0,1.569e22,315000.0,1.569e22,315001.0,0.0,324000.0,0.0
324001.0,1.569e22,327000.0,1.569e22,327001.0,0.0,336000.0,0.0
336001.0,1.569e22,339000.0,1.569e22,339001.0,0.0,348000.0,0.0
348001.0,1.569e22,351000.0,1.569e22,351001.0,0.0,360000.0,0.0,end
$ (2) Flux history of T in Enclosure 1
0.0,1.414e22,3000.0,1.414e22,3001.0,0.0,12000.0,0.0
12001.0,1.414e22,15000.0,1.414e22,15001.0,0.0,24000.0,0.0
24001.0,1.414e22,27000.0,1.414e22,27001.0,0.0,36000.0,0.0
36001.0,1.414e22,39000.0,1.414e22,39001.0,0.0,48000.0,0.0
48001.0,1.414e22,51000.0,1.414e22,51001.0,0.0,60000.0,0.0
60001.0,1.414e22,63000.0,1.414e22,63001.0,0.0,72000.0,0.0
72001.0,1.414e22,75000.0,1.414e22,75001.0,0.0,84000.0,0.0
84001.0,1.414e22,87000.0,1.414e22,87001.0,0.0,96000.0,0.0
96001.0,1.414e22,99000.0,1.414e22,99001.0,0.0,108000.0,0.0
108001.0,1.414e22,111000.0,1.414e22,111001.0,0.0,120000.0,0.0
120001.0,1.414e22,123000.0,1.414e22,123001.0,0.0,132000.0,0.0
132001.0,1.414e22,135000.0,1.414e22,135001.0,0.0,144000.0,0.0
```

```
144001.0,1.414e22,147000.0,1.414e22,147001.0,0.0,156000.0,0.0
156001.0,1.414e22,159000.0,1.414e22,159001.0,0.0,168000.0,0.0
168001.0,1.414e22,171000.0,1.414e22,171001.0,0.0,180000.0,0.0
180001.0,1.414e22,183000.0,1.414e22,183001.0,0.0,192000.0,0.0
192001.0,1.414e22,195000.0,1.414e22,195001.0,0.0,204000.0,0.0
204001.0,1.414e22,207000.0,1.414e22,207001.0,0.0,216000.0,0.0
216001.0,1.414e22,219000.0,1.414e22,219001.0,0.0,228000.0,0.0
228001.0,1.414e22,231000.0,1.414e22,231001.0,0.0,240000.0,0.0
240001.0,1.414e22,243000.0,1.414e22,243001.0,0.0,252000.0,0.0
252001.0,1.414e22,255000.0,1.414e22,255001.0,0.0,264000.0,0.0
264001.0,1.414e22,267000.0,1.414e22,267001.0,0.0,276000.0,0.0
276001.0,1.414e22,279000.0,1.414e22,279001.0,0.0,288000.0,0.0
288001.0,1.414e22,291000.0,1.414e22,291001.0,0.0,300000.0,0.0
300001.0,1.414e22,303000.0,1.414e22,303001.0,0.0,312000.0,0.0
312001.0,1.414e22,315000.0,1.414e22,315001.0,0.0,324000.0,0.0
324001.0,1.414e22,327000.0,1.414e22,327001.0,0.0,336000.0,0.0
336001.0,1.414e22,339000.0,1.414e22,339001.0,0.0,348000.0,0.0
348001.0,1.414e22,351000.0,1.414e22,351001.0,0.0,360000.0,0.0,end
end of table input
$
$
control input
  time=0.0,end
  tstep=1.0,end
  timend=360000.0,end
  nprint=10,end
  itermx=9000,end
  delcmx=1.0e-7,end
  bump=1.e-3,end
  damp=0.7
  bound=4.0,end
  omega=1.3,end
end of control input
$
$
plot input
  nplot=5,end
  plotseg=1,end
  plotencl=1,2,end
  dname=d,t,end
  ename=d2g,t2g,dtg,end
  dplot=sconc,moblinv,sflux,trapinv,end
  eplot=press,end
end of plot input
$
end of data
```

References

[1] M. Wykes, et al. Hydrogenic inventory minimisation for the ITER torus and neutral beam cryopumps. WORKSHOP ON IN-VESSEL T-INVENTORY, EFDA-JET, 19-21 March 2003.

[2] L. Heikinheimo et al., « Dielectric window development for the ITER ICRF vacuum transmission line" VTT Publications 359.

[3] S. Yamamoto, ITER DDD 5.5M, "Radiation effects", 1998.

[4] F. Wasastjerna,"MCNP4A Calculations of the Neutron and Gamma Flux In and Near an ITER Equatorial Port Containing an ICRH Array"VTT Energy Technical Report RFD-22/96 (1996) 21 pp.

[5] G. R. Longhurst, October 2004, TMAP7 User Manual, INEEL/EXT-04-02352., Idaho National Engineering and Environmental Laboratory, Idaho Falls, Idaho.

[6] L. A. Sedano "CIEMAT Report. Internal Workshop on Tritium Task Activities", March 2004. CIEMAT Rep. Off. (*In press*).

[7] ITER Design Requirements and Guidelines 1&2. (2001)

[8] ITER Design Description Document 5.1 (2001).

[9] W.K. Jones. LA-701 "Thermodynamic functions for tritium deuteride"Series A. Los Alamos National Laboratory Research Library (1948)

[10] J.F. Ziegler, SRIM-2003, www.srim.org.

[11] J.D. Fowler, D. Chandra, T.S. Elleman, A.W. Payne, K. Verghese, "Tritium Diffusion in Al_2O_3 and BeO", J. Am. Ceram. Soc. 60 3-4 (1977) 155.

[12] R.M. Roberts, T.S. Elleman, H. Palmour III, K. Verghese,"Hydrogen Permeability of Sintered Aluminium Oxide",. Am. Ceram. Soc. 62 (1979) 495.

[13] Gervasini G. and Reiter F. "Tritium-Material Interaction if First Walls and Plasma Facing Components of Fusion Reactors" Proc. International Workshop on Physics and Technology of Tritium for Fusion Reactors, Varenna, Italy, September 6-14, 1993 Transaction of Fusion Technology, 27, 2T, FUSTE8, 30 (1995).

[14] E. Serra, G. Benamati and O. V. Ogorodnikova, "Hydrogen isotopes transport parameters in fusion reactor materials" , J. of Nucl. Mater. 255 (1998) 105-115.

[15] R.G. Macaulay-Newcombe, D.A. Thompson, "Ion beam analysis of deuterium-implanted Al_2O_3 and tungsten" J. of Nucl. Mater.258-263 (1998) 1109-1113

[16] L. A. Sedano *et al.*, "Ionising effects on D_2 permeability through aluminae". Proc. of 7th Int. Symp. on Fusion Nucl. Techn, May 22-27, 2005 Tokyo.